# Comparison of Neural Network NARMA-L2 Model Reference and Predictive Controllers for Electromagnetic Space Vehicle Suspension System

Mustefa Jibril, Messay Tadese and Nuriye Hassen
*School of Electrical and Computer Engineering, Dire Dawa Institute of Technology, Dire Dawa, Ethiopia*

**Abstract:** Electromagnetic Suspension System (EMS) is mostly used in the field of high-speed vehicle. In this study, a space exploring vehicle quarter electromagnetic suspension system is modelled, designed and simulated using Neural network-based control problem. NARMA-L2, Model reference and predictive controllers are designed to improve the body travel of the vehicle using bump road profile. Comparison between the proposed controllers is done and a promising simulation result have been analyzed.

## INTRODUCTION

Electromagnetic Suspension (EMS) is the magnetic levitation of an object achieved by constantly altering the strength of a magnetic field produced by electromagnets using a feedback loop. In most cases the levitation effect is mostly due to permanent magnets as they don't have any power dissipation with electromagnets only used to stabilize the effect.

According to Earnshaw's Theorem a paramagnetically magnetized body cannot rest in stable equilibrium when placed in any combination of gravitational and magnetostatic fields. In these kinds of fields an unstable equilibrium condition exists. Although, static fields cannot give stability, EMS works by continually altering the current sent to electromagnets to change the strength of the magnetic field and allows a stable levitation to occur. In EMS a feedback loop which continuously adjusts one or more electromagnets to correct the object's motion is used to cancel the instability.

Many systems use magnetic attraction pulling upwards against gravity for these kinds of systems as this gives some inherent lateral stability but some use a combination of magnetic attraction and magnetic repulsion to push upwards. Magnetic levitation technology is important because it reduces energy consumption, largely obviating friction. It also avoids wear and has very low maintenance requirements. The application of magnetic levitation is most commonly known for its role in Maglev trains.

When a current pass through a wire, a magnetic field around that wire is generated. The strength of the generated magnetic field is proportional to the current through the wire. When a wire is coiled, this generated magnetic field is concentrated through the center of the coil. The strength of this field can be greatly increased by placing a ferromagnetic material in the center of the coil. This field is easily manipulated by passing a varying current in the wire. Therefore, a combination of permanent magnets with electromagnets is an optimal arrangement for levitation purposes[1]. To reduce average power requirements, often the electromagnetic suspension is used only to stabilize the levitation and the static lift against gravity is provided by a secondary permanent magnet system, often pulled towards a relatively inexpensive soft ferromagnetic material such as iron or steel.
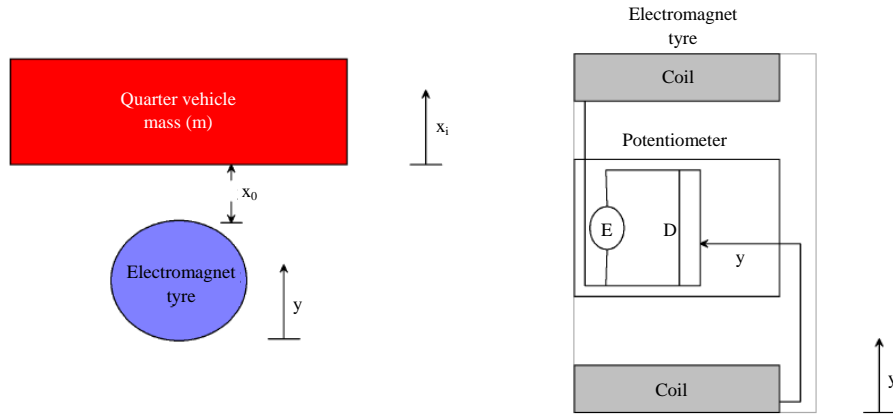
Fig. 1: Quarter vehicle electromagnetic suspension system and the electromagnetic tire design

## MATERIALS AND METHODS

**Mathematical modelling of the electromagnetic suspension system:** Figure 1 shows a quarter vehicle electromagnetic suspension system and the electromagnetic tire design[2].

The tire is suspended with an initial length x0 for an initial current i0. The electromagnet tire has a potentiometer fixed inside it and at the layer of the tire there is a coil connected. The potentiometer has a source voltage E and a resistor length D. When a road disturbance is accrued, the tire with the attached potentiometer rod will move upward and downward with a length y, so, the metallic body mass will move. The design is as follows. Apply Kirchhoff's voltage equation for the electric circuit[3]:

$$V = V_R + V_L \Rightarrow u(t) = iR + L\frac{di}{dt} \qquad (1)$$

where u, I, R and L is applied voltage input, current in the electromagnet coil, coil's resistance and coil's inductance, respectively. Energy stored in the inductor can be written as:

$$W_{IStored} = \frac{1}{2}Li^2 \qquad (2)$$

Since, power in electrical system ($P_e$) = Power in the mechanical system ($P_m$) where:

$$P_e = \frac{dW_{IStored}}{dt}$$

and:

$$P_m = -f_m \frac{dx}{dt}$$

therefore:

$$f_m = -\frac{dW_{IStore}}{dt}\frac{dt}{dx} = -\frac{dW_{IStore}}{dx} \qquad (3)$$

where $f_m$ is known as electromagnet force now substituting (Eq. 2) in Eq. 3:

$$\begin{aligned} f_m &= -\frac{d}{dx}\left(\frac{1}{2}Li^2\right) \\ &= -\frac{1}{2}i^2\frac{d}{dx}(L) \end{aligned} \qquad (4)$$

Since, the inductance L is a nonlinear function of body travel position (x), we shall neglect the leakage flux and eddy current effects (for simplicity), so that, the inductance varies with the inverse of body travel position as follows:

$$L = \frac{K}{x} \quad \text{where in} \quad K = \frac{\mu_0 N^2 A}{2} \qquad (5)$$

Where:
$\mu_0$ = The inductance constant
A = The pole area
N = The number of coil turns
K = Electromagnet force constant

$$\begin{aligned} f_m &= -\frac{1}{2}i^2\frac{d}{dx}\left(\frac{k}{x}\right) \\ &= -\frac{1}{2}i^2\left(-\frac{k}{x^2}\right) \\ \therefore f_m &= \frac{K}{2}\left(\frac{i^2}{x^2}\right) \end{aligned} \qquad (6)$$

If $f_m$ is electromagnetic force produced by input current, $f_g$ is the force due to gravity and f is net force acting on the vehicle body, the equation of force can be written as[4]:

$$f_g = f_m + f$$
$$= f_m + m\left(\frac{d^2x}{dt^2}\right)$$
$$\Rightarrow m\frac{dv}{dt} = f_g - f_m = mg - \frac{K}{2}\left(\frac{i(t)}{x(t)}\right)^2 \quad (7)$$

where, m = vehicle mass and v = dx/dt = dh/dt which is velocity of the vehicle body movement. At equilibrium the force due to gravity and the magnetic force are equal and oppose each other so that the vehicle body levitates. i.e., $f_g = -f_m$ and f = 0. On the basis of electro-mechanical modeling, the nonlinear model of magnetic levitation system can be described as follows: The general form of an affine system[5]:

$$\frac{dz}{dt} = f(z) + g(z).u \quad (8)$$

Is obtained by denoting variables for state space representation as follows:

$$z_1 = x$$
$$z_2 = \frac{dx}{dt} = v$$
$$z_3 = i \quad (9)$$

Substitute Eq. 9 or the state variables in to Eq. 1 and Eq. 7:

$$u(t) = z_3.R + L.x\dot{z}_3$$
$$m\dot{z}_2 = m.g - \frac{K}{2}\left(\frac{z_3}{z_1}\right)^2 \quad (10)$$

Then, the nonlinear state space model is:

$$\dot{z}_1 = x_2$$
$$\dot{z}_2 = \left(g - \frac{K}{2m}\right)\left(\frac{z_3}{z_1}\right)^2$$
$$\dot{z}_3 = \frac{u}{L} - z_3\frac{R}{L} \quad (11)$$

The $f_m$ is electromagnetic force produced by input current is related to the current and the road disturbance displacement will be:

$$f_m = g(x,i) \quad (12)$$

Using Taylor series linearization technique, we have:

$$f_m = \left(\frac{\partial g}{\partial x}\right)_{x_0,i_0} x + \left(\frac{\partial g}{\partial i}\right)_{x_0,i_0} i = -\frac{2ki_0^2}{x_0^3}x + \frac{2ki_0}{x_0^2}i \quad (13)$$

where, g = g(x, i) and $(x_0, i_0)$ is the operating point's initial inputs. The applied force to the mass become:

$$M\frac{d^2x}{dt^2} = f_m = -\frac{2ki_0^2}{x_0^3}x + \frac{2ki_0}{x_0^2}i \quad (14)$$

Then, the linearized state space model becomes:

$$\begin{pmatrix} \dot{z}_1 \\ \dot{z}_2 \\ \dot{z}_3 \end{pmatrix} = \begin{pmatrix} 0 & 1 & 0 \\ -\frac{2ki_0^2}{mx_0^3} & 0 & \frac{2ki_0}{mx_0^2} \\ 0 & 0 & -\frac{R}{L} \end{pmatrix} \begin{pmatrix} z_1 \\ z_2 \\ z_3 \end{pmatrix} + \begin{pmatrix} 0 \\ 0 \\ \frac{1}{L} \end{pmatrix} v$$

$$y = (1\ 0\ 0)\begin{pmatrix} z_1 \\ z_2 \\ z_3 \end{pmatrix}$$

From the potentiometer:

$$v = E\frac{y}{D} \quad (15)$$

So, the final state space model becomes:

$$\begin{pmatrix} \dot{z}_1 \\ \dot{z}_2 \\ \dot{z}_3 \end{pmatrix} = \begin{pmatrix} 0 & 1 & 0 \\ -\frac{2ki_0^2}{mx_0^3} & 0 & \frac{2ki_0}{mx_0^2} \\ 0 & 0 & -\frac{R}{L} \end{pmatrix} \begin{pmatrix} z_1 \\ z_2 \\ z_3 \end{pmatrix} + \begin{pmatrix} 0 \\ 0 \\ \frac{E}{LD} \end{pmatrix} y$$

$$y = (1\ 0\ 0)\begin{pmatrix} z_1 \\ z_2 \\ z_3 \end{pmatrix}$$

The system parameters are shown in Table 1. The transfer function become:

$$\frac{X(s)}{Y(s)} = \frac{1}{s^3 + 50s^2 + 0.1375s + 6.874}$$

Table 1: System parameters

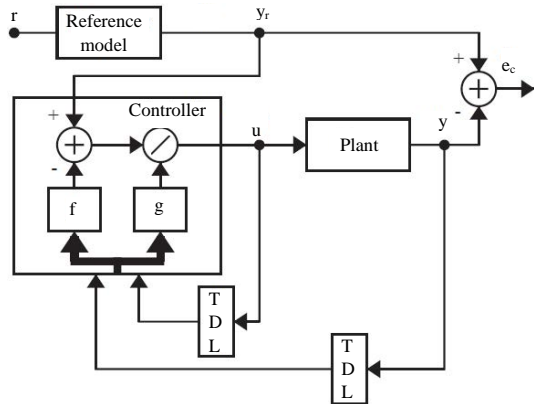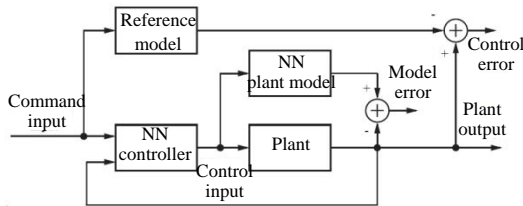| Parameters | Symbols | Values |
|---|---|---|
| Mass of the vehicle | m | 1 (kg) |
| Coil resistance | R | 10 (Ω) |
| Coil inductance | L | 0.2 (H) |
| Initial current | $i_0$ | 0.8 (A) |
| Initial displacement | $x_0$ | 0.03 (m) |
| Electromagnet constant | k | $2.9\times10^{-6}$ Nm$^2$/A$^2$ |
| Potentiometer voltage | E | 5 (V) |
| Potentiometer distance | D | 0.13 (m) |

Fig. 2: NARMA-L2 controller



Fig. 3: Model reference control architecture

**The proposed controller design**
**NARMA-L2 controller design:** One of the main features of the NARMA-L2 neurocontroller is to transform nonlinear system dynamics into linear dynamics by canceling the nonlinearities. We begin by describing how the identified neural network model can be used to design a controller. The advantage of the NARMA-L2 form is that you can solve for the control input that causes the system output to follow a reference signal (Fig. 2)[6].

**Model reference controller design:** The model reference controller is designed to contain two neural networks: a neural network controller and a neural network plant model as shown in Fig. 3. The plant model is identified first and then the controller is trained, so that, the plant output follows the reference model output.

**Predictive controller design:** There are different types of neural network predictive controller that are based on linear model controllers. The proposed neural network predictive controller uses a neural network model of a nonlinear plant to predict future plant performance. The proposed controller then calculates the control input that will optimize plant performance over a specified future time horizon. The primary goal of the model predictive control is to determine the neural network plant model. Then, the plant model is used by the controller to predict future performance. The process is represented by Fig. 4.
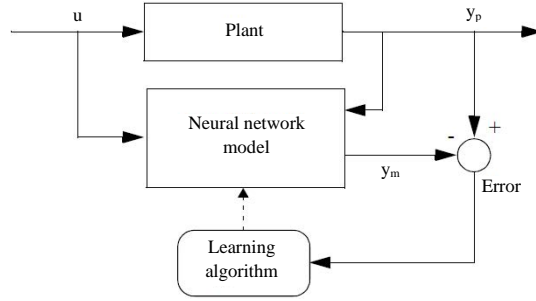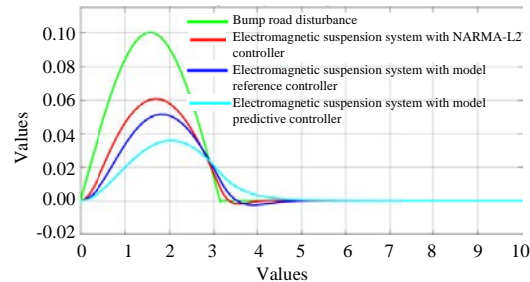


Fig. 4: Plant identification



Fig. 5: Body travel response for a bump road disturbance

Table 2: Numerical values of the body travel simulation output

| Systems | Bump (m) |
|---|---|
| Road profile | 0.100 |
| NARMA-L2 | 0.061 |
| Model reference | 0.047 |
| Predictive | 0.038 |

**RESULTS AND DISCUSSION**

**Body travel output specification:** One of the major specifications of a suspension system is whatever the road disturbance input, the best design performance of the body travel vertical displacement is to approach to zero.

**Comparison of a quarter vehicle electromagnetic suspension system with LQG and LQI controllers for a bump road disturbance:** The quarter vehicle electromagnetic suspension system with the proposed controller's comparison for a 10 cm bump road disturbance input simulation result for body travel response is shown in Fig. 5. The simulation result numerical value is shown in Table 2. Table 2 shows that the quarter vehicle electromagnetic suspension system with Predictive controller body travel is minimum and improved the road handling criteria[7].

**CONCLUSION**

In this study, a quarter vehicle electromagnetic suspension system design and analysis have been done

using MATLAB/Simulink. In order to increase the performance of the electromagnetic suspension system, Neural network-based control technique is used. The main aim of this paper is to control the vehicle body travel based on road disturbance input. Comparison of the quarter vehicle electromagnetic suspension system with NARMA-L2, model reference and predictive controllers to improve the performance of the body travel output using a bump, random and sinusoidal road profiles. The quarter vehicle electromagnetic suspension system with Predictive controller body travel is minimum and improved the road handling criteria[8].

## REFERENCES

01. Katarne, R. and S. Sharma, 2019. Active hybrid suspension system: A review. Proceedings of the 2nd International Conference on Emerging trends in Manufacturing, Engines and Modelling (ICEMEM-2019), Vol. 810, December 23-24, 2019, IOP, Mumbai, India, pp: 1-9.

02. Agrawal, P., A. Desai, J.S. Mallireddy and K.P. Wani, 2019. Design and development of a semi active electromagnetic suspension system (No. 2019-28-0110). SAE Technical Paper, SAE International, Warrendale, Pennsylvania.

03. Qin, Y., F. Zhao, Z. Wang, L. Gu and M. Dong, 2017. Comprehensive analysis for influence of controllable damper time delay on semi-active suspension control strategies. J. Vibr. Acoust., Vol. 139, No. 3. 10.1115/1.4035700

04. Yadav, S., 2018. Review on design & fabrication of magnetic suspension. Int. J. Innovative Res. Sci. Eng. Technol., 7: 10823-10827.

05. Chen, L., D. Shi, R. Wang and H. Zhou, 2016. Energy conservation analysis and control of hybrid active semiactive suspension with three regulating damping levels. Shock Vib., Vol. 2016, 10.1155/2016/6196542

06. Peng, M., X. Guo, J. Zou and C. Zhang, 2016. Simulation study on vehicle road performance with hydraulic electromagnetic energy-regenerative shock absorber (No. 2016-01-1550). SAE Technical Paper, Wuhan University of Technology, Wuhan, China.

07. Montazeri-Gh, M. and O. Kavianipour, 2014. Investigation of the active electromagnetic suspension system considering hybrid control strategy. Proc. Inst. Mech. Eng. Part C. J. Mech. Eng. Sci., 228: 1658-1669.

08. Hsieh, C.Y., M. Moallem and F. Golnaraghi, 2015. A bidirectional boost converter with application to a regenerative suspension system. IEEE Trans. Veh. Technol., 65: 4301-4311.